

논문 2015-52-4-7

# RF MOSFET의 바이어스 종속 게이트-드레인 오버랩 캐패시턴스의 새로운 SPICE 모델링

( New SPICE Modeling for Bias-Dependent Gate-Drain Overlap  
Capacitance in RF MOSFETs )

이 상 준\*, 이 성 현\*\*

( Sangjun Lee and Seonghearn Lee<sup>©</sup> )

## 요 약

기존의 BSIM4 모델과 다이오드를 사용한 BSIM4 Macro 모델의 바이어스 종속 게이트-드레인 오버랩 캐패시턴스  $C_{gdo}$  시뮬레이션의 부정확성에 대하여 자세히 분석하였다. 이러한 Macro 모델은 기존의 BSIM4 모델보다 더 정확하지만 선형영역에서 사용될 수 없음을 발견하였다. 기존 모델들의 부정확성을 제거하기 위해서 물리적인 바이어스 종속  $C_{gdo}$  모델 방정식을 사용한 새로운 BSIM4 Macro 모델을 제안하였고 전체 바이어스 영역에서 유효함을 입증하였다.

## Abstract

The inaccuracy of the bias-dependent gate-drain overlap capacitance  $C_{gdo}$  simulation in original BSIM4 and BSIM4 macro model using a diode is analyzed in detail. It is found that the accuracy of the macro model is better than of the BSIM4. However, the macro model cannot be used in the linear region. In order to remove the inaccuracy of the conventional models, a new BSIM4 macro model with a physical bias-dependent  $C_{gdo}$  equation is proposed and its accuracy is validated in the full bias range.

**Keywords** : MOSFET, RF, Modeling, SPICE model, overlap capacitance

## I. Introduction

For the accurate design of RF integrated circuits (ICs), it is important that MOSFETs should be modeled at the high-frequency region and wide

voltage range. For accurate modeling of RF MOSFETs, the gate-drain overlap capacitance  $C_{gdo}$  is a very important parameter as the feedback capacitance affecting power gain. An inaccurate  $C_{gdo}$  model can lead to incorrect SPICE simulation results for the cut-off frequency  $f_T$  and the maximum oscillation frequency  $f_{max}$ <sup>[1]</sup>.

Recently, BSIM4<sup>[2]</sup> is widely used as a RF SPICE model of MOSFETs. In the original BSIM4,  $C_{gdo}$  is modeled as the bias-dependent  $CGDL$  in the  $LDD$  (lightly doped drain) region and bias-independent  $CGDO$  in the  $Non-LDD$  region in the gate-drain

\* 학생회원, \*\* 정회원, 한국외국어대학교 전자공학과  
(Department of Electronics Engineering, Hankuk  
University of Foreign Studies)

© Corresponding Author(E-mail: shlee@hufs.ac.kr)

※ 이 연구는 2014학년도 한국외국어대학교 교내 학술  
연구비의 지원에 의하여 이루어진 것임.

Received ; December 1, 2014 Revised ; March 10, 2015

Accepted ; March 30, 2015

overlap region. However, when the drain-gate voltage  $V_{dg}$  ( $= V_{ds} - V_{gs}$ ) for N-MOSFETs is in the negative range, the BSIM4 is unable to model  $C_{gdo}$ .

In order to improve the original BSIM4, a BSIM4 macro model adding the gate-drain junction diode  $D_{gdo}$ <sup>[3]</sup> has been used for a N-MOSFET in Fig. 1(a). The bias-dependent  $C_{gdo}$  due to the depleted  $n^-$ -LDD below the oxide layer in the gate-drain overlap region in the positive  $V_{dg}$  is modeled by adding  $D_{gdo}$ . However,  $D_{gdo}$  is unable to model  $C_{gdo}$  in the negative  $V_{dg}$ . In particular, the macro model does not work in the linear region of  $V_{dg} < -V_{th}$  because  $D_{gdo}$  turns on.

In order to model  $C_{gdo}$  in the negative  $V_{dg}$  accurately in this paper, an improved bias-dependent  $C_{gdo}$  equation is constructed by modeling a parasitic MOS capacitor in the gate-drain overlap LDD region.

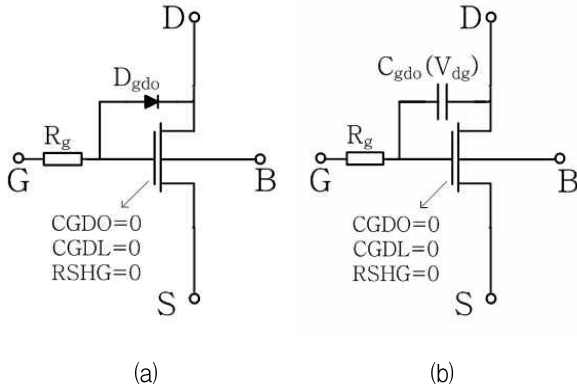


그림 1. 두 가지 BSIM4 macro MOSFET 모델.  $C_{gdo}$ 와  $R_g$ 의 내부 값을 제거하기 위하여 BSIM4 파라미터  $CGDO$ ,  $CGDL$ 과  $RSHG$ 가 0으로 설정됨  
(a) 다이오드를 사용한 BSIM4 macro N-MOSFET 모델  
(b) 바이어스 종속  $C_{gdo}$ 를 사용한 새로운 BSIM4 macro 모델

Fig 1. Two BSIM4 macro MOSFET models. The BSIM4 parameters of  $CGDO$ ,  $CGDL$ , and  $RSHG$  are set to zero to eliminate the internal values of  $C_{gdo}$  and  $R_g$ .  
(a) A BSIM4 macro model using a diode for N-MOSFET.  
(b) A new BSIM4 macro model using a bias-dependent  $C_{gdo}$ .

## II. Modeling and Analysis

### 1. $C_{gdo}$ Measurement

S-parameters are measured on multi-finger N-MOSFETs with the gate length ( $L_g = 0.18\mu\text{m}$ ), the gate finger number ( $N_f = 16$ ) and the unit finger width ( $W_u = 5\mu\text{m}$ ). An accurate de-embedding procedure was carried out to remove pad and interconnection parasitics from measured S-parameters<sup>[4]</sup>.

After the drain, source and substrate resistances are determined by using a RF direct extraction method<sup>[5-6]</sup> and the gate resistance is extracted from a non-quasi-static model<sup>[7]</sup>, intrinsic  $Y^i$ -parameters are determined by subtracting them from measured S-parameters. Using  $Y_{12}^i$ -parameter in the low-frequency(LF) region,  $C_{gdo}$  in the saturation region is extracted by<sup>[6]</sup>:

$$C_{gdo} \approx -\frac{1}{\omega} \text{Imag}(Y_{12}^i)_{LF} \quad (1)$$

Fig. 2 shows (1) versus frequency along the wide variation of  $V_{gs}$  at  $V_{ds} = 1\text{V}$  for a N-MOSFET. Since the surface depletion width in the gate-drain overlap  $n^-$ -LDD region decreases with increasing  $V_{gs}$ ,  $C_{gdo}$  increases.

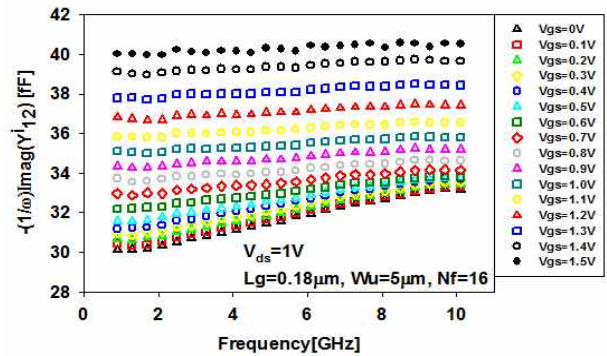


그림 2.  $V_{gs}$  변화에 따라 추출된  $(-1/\omega)\text{Imag}(Y_{12}^i)$  대 주파수 그래프

Fig 2. Extracted  $(-1/\omega)\text{Imag}(Y_{12}^i)$  values versus frequency at various  $V_{gs}$ .

## 2. Analysis of Conventional Models

In Fig. 3,  $C_{gdo}$  values extracted from Fig. 2 in the low-frequency region are plotted as a function of  $V_{dg}$  with those of the original BSIM4 and BSIM4 macro model using  $D_{gdo}$ . Since the surface of  $n^-$ -LDD region under the oxide layer begins to be depleted from  $V_{dg}$  of flat-band voltage  $V_{FBO}$  in the drain overlap region for N-MOSFET,  $C_{gdo}$  decreases with increasing  $V_{dg}$  in the saturation region of  $V_{dg} > -V_{th}$  at  $V_{th}=0.46V$ . The measurement data at  $V_{dg} < -0.46$  V are excluded in Fig. 3, because the channel capacitance in the linear region is included in the data.

The BSIM4 drain overlap capacitance is modeled by the differential  $dQ_{overlap,d}/dV_{gd}$  of the following charge equation<sup>[2]</sup>:

$$\frac{Q_{overlap,d}}{W_{active}} = CGDO \cdot V_{gd} + CGDL \left[ V_{gd} - V_{gd,overlap} - \frac{CKAPPAD}{2} \left( -1 + \sqrt{1 - \frac{4V_{gd,overlap}}{CKAPPAD}} \right) \right] \quad (2)$$

$$V_{gd,overlap} = \frac{1}{2} \left( V_{gd} + \delta_1 - \sqrt{(V_{gd} + \delta_1)^2 + 4\delta_1} \right) \quad (3)$$

where  $\delta_1 = 0.02V$

where  $CKAPPAD$  is defined as the coefficient of bias-dependent overlap capacitance for the drain side.

The decreasing surface depletion capacitance at the

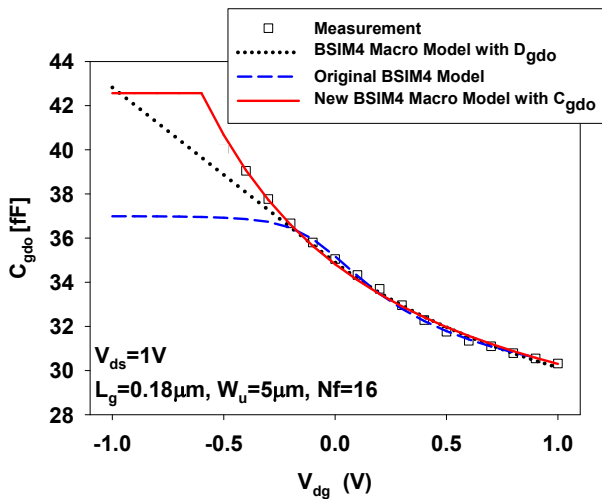


그림 3. N-MOSFET의 측정값과 모델된  $C_{gdo}$  대  $V_{dg}$   
Fig 3. Measured and modeled  $C_{gdo}$  versus  $V_{dg}$  for N-MOSFET.

positive  $V_{dg}(= -V_{gd})$  in Fig. 3 can be modeled by fitting  $dQ_{overlap,d}/dV_{dg}$  of (2). However,  $C_{gdo}$  becomes saturated in the range of  $V_{dg} < -0.2V$  because  $V_{gd,overlap}$  of (3) rapidly approaches to zero with decreasing  $V_{dg}(= -V_{gd})$  in the negative range. Thus, the BSIM4 drain overlap capacitance model shows the substantial disagreement with the measurement data below  $V_{dg} = -0.2V$  in Fig. 3.

For the BSIM4 macro model using  $D_{gdo}$ <sup>[3]</sup> in Fig. 1(a), the junction diode  $C_{gdo}$  equation is defined by<sup>[8]</sup>:

$$C_{gdo} = \frac{C_{jo}}{\left[ 1 + \left( \frac{V_{dg}}{V_j} \right)^{M_j} \right]} \quad \text{for } V_{dg} > 0 \quad (4)$$

$$C_{gdo} = C_{jo} \left[ 1 - M_j \left( \frac{V_{dg}}{V_j} \right) \right] \quad \text{for } V_{dg} < 0 \quad (5)$$

where  $C_{jo}$ ,  $M_j$  and  $V_j$  are defined as the junction capacitance at zero-bias, the grading coefficient and built-in voltage, respectively. Although (4) and (5) are physically unacceptable for a parasitic MOS capacitor in the gate-drain overlap LDD region, these can be used for an empirical model.

The surface depletion capacitance decreased at  $V_{dg} > 0$  is accurately fitted by (4) in Fig. 3. However, the depletion capacitance at  $V_{FBO} < V_{dg} < 0V$  in Fig. 3 can not be modeled by the linear dependent equation of (5).

Theoretically,  $C_{gdo}$  is unchanged as the oxide capacitance  $C_{OLD}$  over the drain overlap region at  $V_{dg} \leq V_{FBO}$ , because the surface of  $n^-$ -LDD in the gate-drain overlap region is accumulated. Thus, the linear equation of (5) is unable to model the bias-independent  $C_{gdo}$  at  $V_{dg} \leq V_{FBO}$ .

## 3. New BSIM4 Macro Modeling

In order to overcome the problems of the conventional models, a physical bias-dependent  $C_{gdo}$  model is newly developed in this work. The new  $C_{gdo}$  model parameters are represented in Fig. 4.  $L_{OV}$  is

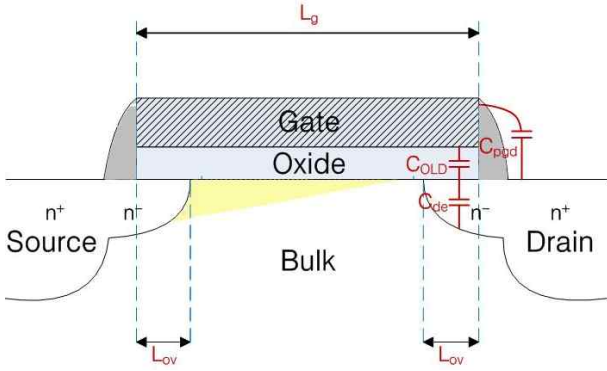


그림 4. 새로운 BSIM4 오버랩 캐패시턴스 모델의 파라미터 성분들을 나타낸 포화영역에서의 MOSFET 단면도

Fig 4. Schematic diagram of a MOSFET structure in the saturation region to explain overlap capacitance model parameters in a new BSIM4 macro model

defined as the drain overlap length at the drain overlap  $LDD$  region.

In a parasitic MOS capacitor in the gate-drain overlap  $n^- - LDD$  region, the oxide capacitance  $C_{OLD}$  is connected in series with the surface depletion capacitance  $C_{de}$  in the drain  $LDD$  region<sup>[9]</sup>. Together with the series capacitances, the parasitic gate-drain capacitance  $C_{pgd}$  occurring to the exterior of the drain  $LDD$  region is connected in parallel<sup>[9]</sup>.

Thus, a physical bias-dependent  $C_{gdo}$  model is expressed as:

$$C_{gdo} = \frac{C_{OLD} \cdot C_{de}}{C_{OLD} + C_{de}} + C_{pgd} \quad (6)$$

In this work, the depletion capacitance at the surface of the  $LDD$  region is modeled by:

$$C_{de} = C_o \left( 1 - \frac{V_{dg}}{V_{FBO}} \right)^{-M} \quad \text{for } V_{dg} > V_{FBO} \quad (7)$$

where  $V_{FBO}$  is a negative number for N-MOSFETs, and  $C_o$  and  $M$  are defined as the zero-bias capacitance and the grading coefficient, respectively. This capacitance is generated by the expansion of the depleted surface layer of  $n^- - LDD$  region due to more band bending at higher  $V_{dg}$ <sup>[9]</sup>.

Since  $C_{OLD}$  is independent of the bias and  $C_{de}$  is reduced with increasing  $V_{dg}$ ,  $C_{gdo}$  decreases as shown in Fig. 3. If  $C_{de}$  in (6) is significantly decreased until  $C_{de} \ll C_{OLD}$  at very high  $V_{dg}$ , (6) is reduced by:

$$C_{gdo} \approx C_o \left( 1 - \frac{V_{dg}}{V_{FBO}} \right)^{-M} + C_{pgd} \quad (8)$$

Thus,  $C_{pgd}$  of 24.16fF is accurately extracted by fitting (8) to  $C_{gdo}$  data at  $V_{dg} = 0.7 \sim 1V$ . When the  $n^- - LDD$  region is accumulated at  $V_{dg} \leq V_{FBO}$ ,  $C_{gdo}$  is determined by  $C_{OLD} + C_{pgd}$ . However,  $C_{OLD}$  is unable to be directly extracted from measured  $C_{gdo}$  data at  $V_{dg} \leq V_{FBO}$ , because the channel capacitance  $C_{CC}$  is added in the linear region ( $V_{dg} < -V_{th}$ ). Thus,  $C_{OLD}$  needs to be independently extracted using another method.

In order to extract  $C_{OLD}$ , the oxide capacitance per unit area  $C_{OX}$  is accurately extracted by the following equation at  $V_{ds} = 0V$ :

$$C_{OX} = \frac{C_G - C_{PG}}{NF \cdot W_u \cdot (L_g - 2L_{OV})} \quad (9)$$

where  $C_{PG}$  is the extrinsic parasitic capacitance outside the channel area at  $V_{ds} = 0V$ .

The total gate capacitance  $C_G$  at  $L_g$  is extracted by using the data of  $(-2/\omega) \text{Imag}(Y_{12}^i)_{LF}$  at  $V_{ds} = 0V$  and  $V_{gs} = 0.7V$  under the assumption of symmetric source and drain for the N-MOSFETs<sup>[10]</sup>.

In order to determine  $L_{OV}$ , a RF direct extraction method<sup>[11]</sup> is applied as follows: The gate-bulk capacitance  $C_{gb}$  in the low-frequency region is determined by:

$$C_{gb} \approx \frac{1}{\omega} \text{Imag}(Y_{11}^i + 2Y_{12}^i)_{LF} \quad (10)$$

Since the inversion charge layer totally shields the intrinsic bulk region from the gate, the intrinsic gate-bulk capacitance  $C_{GBI}$  in the channel area is masked due to the inversion region at  $V_{gs} > V_{th}$ . Thus, the extrinsic gate-bulk capacitance  $C_{GBE}$  is

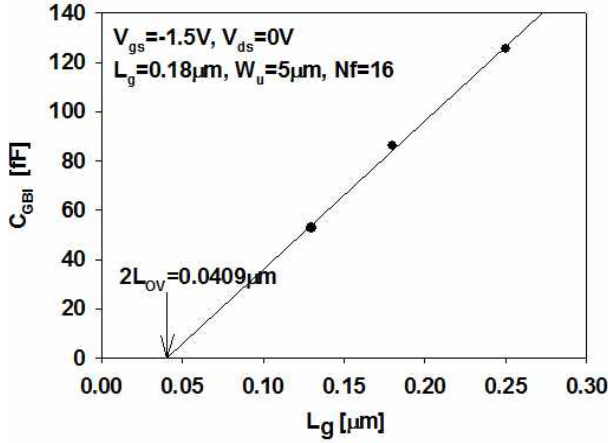


그림 5. 추출된  $C_{GBI}$  대  $L_g$  데이터와 피팅 선  
Fig 5. Extracted values and their regression line of  $C_{GBI}$  versus  $L_g$ .

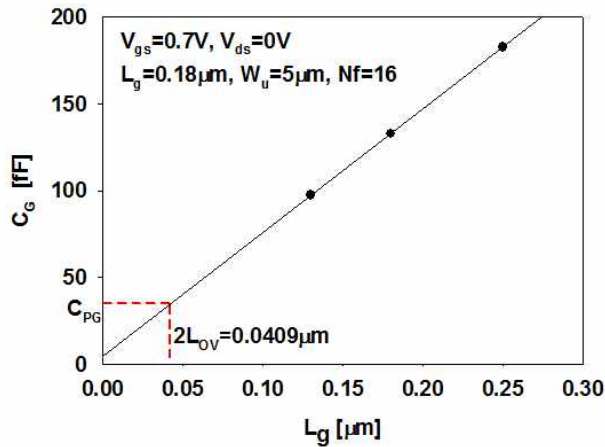


그림 6. 추출된  $C_G$  대  $L_g$  데이터와 피팅 선  
Fig 6. Extracted values and their regression line of the  $C_G$  versus  $L_g$ .

accurately extracted by (10) at  $V_{gs} > V_{th}$ . In this method,  $C_{GBI}$  is extracted by subtracting (10) at  $V_{gs} = 0.6V$  and  $V_{ds} = 0V$  from (10) at  $V_{gs} = -1.5V$  and  $V_{ds} = 0V$ . As shown in Fig. 5,  $L_{OV}$  is determined from the x-intercept of a linear regression line for  $C_{GBI}$  vs.  $L_g$  at  $V_{gs} = -1.5V$  that is the flat band voltage of the channel region.

In order to extract the oxide capacitance  $C_G - C_{PG}$  in the channel area in (9),  $C_{PG}$  is determined from  $C_G$  value at  $L_g = 2L_{OV}^{[10]}$  as shown in Fig. 5. After  $C_{OX}$  is extracted by substituting  $C_{PG}$  and  $L_{OV}$  into

(9),  $C_{OLD}$  is calculated by  $C_{OX} \cdot NF \cdot W_u \cdot L_{OV}$ .

In order to extract  $M$ ,  $C_o$  and  $V_{FBO}$  accurately, (6) at  $V_{dg} \geq V_{FBO}$  is rewritten by:

$$\frac{1}{C_{gdo} - C_{pgd}} = \frac{1}{C_{OLD}} + \frac{1}{C_{de}} \quad (11)$$

$$= \left[ \frac{1}{C_{OLD}} + \frac{1}{C_o} \left( 1 - \frac{V_{dg}}{V_{FBO}} \right)^M \right]$$

The values of  $V_{FBO} = -0.6V$ ,  $C_o = 25.3fF$  and  $M = 1.03$  are extracted by fitting (11) to  $1/(C_{gdo} - C_{pgd})$  data in the saturation region of  $V_{dg} \geq -0.5V$ .

For HSPICE modeling, a following bias-dependent  $C_{gdo}$  equation is constructed by:

$$C_{gdo} = \frac{1}{\frac{1}{C_{OLD}} + \frac{1}{C_o} \left( \frac{1 + \text{sgn}(V_{dg} - V_{FBO})}{2} \right) \left( 1 - \frac{V_{dg}}{V_{FBO}} \right)^M} + C_{pgd} \quad (12)$$

where the  $\text{sgn}(x)$  function ( $= 1$  at  $x > 0$ ,  $0$  at  $x=0$ ,  $-1$  at  $x < 0$ ) is a HSPICE built-in function<sup>[8]</sup> used to define the effective range of  $V_{dg} \geq V_{FBO}$  in (7).

#### 4. Accuracy Analysis of the New Model

As shown in Fig. 3, a modeled  $C_{gdo}$  curve of Fig. 1(b) using (12) exhibits better agreement with the measurement data than the conventional ones. Unlike the conventional models, the new macro model with  $C_{gdo}$  provides a more accurate overlap capacitance simulation in the range of  $V_{dg} < 0$  by modeling a parasitic MOS capacitor in the gate-drain overlap region physically.

As shown in Fig. 7 and table I, in order to confirm the RF accuracy of the new BSIM4 macro model with a bias-dependent  $C_{gdo}$  in Fig. 1(b), frequency-dependent power gain Gmax curves and average Gmax errors for the new and conventional models are compared with measurement data at  $V_{gs} = 1.4V$  and  $V_{ds} = 1V$ . The modeled Gmax values and errors of the conventional models is much larger than those of the new one, because  $C_{gdo}$  is underestimated in the original one. Although the BSIM4 macro model

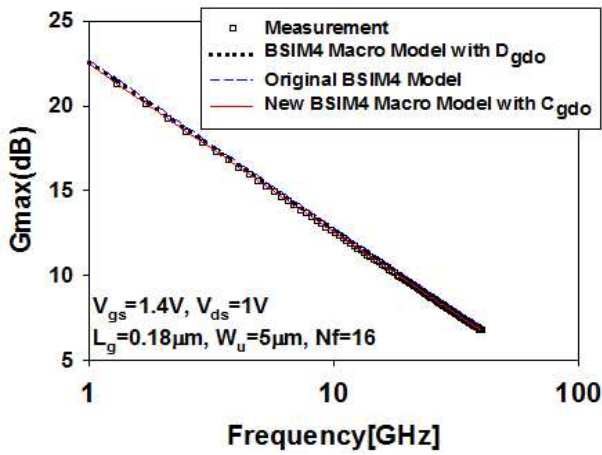


그림 7. 측정값과 모델된 주파수 종속 전력 종속 곡선  
Fig 7. Measured and modeled frequency-dependent power gain curves.

표 1. 측정값과 모델된 주파수 종속 전력종속 곡선 데이터의 에러율 ( $V_{gs}=1.4V$  and  $V_{ds}=1V$ )  
Table 1. The average errors of measured and modeled frequency-dependent power gain curves data ( $V_{gs}=1.4V$  and  $V_{ds}=1V$ ).

Models	Average $G_{max}$ Error (%)
Original BSIM4 model	5.99
BSIM4 macro model with $D_{gdo}$	2.63
New BSIM4 macro model with $C_{gdo}$	0.18

\* Average  $G_{max}$  Error (%) =

$$\frac{100}{N} \sum_f \left| \frac{\text{measured } G_{max} - \text{modeled } G_{max}}{\text{measured } G_{max}} \right|$$

where N is the number of frequency f

with a diode shows the better agreement than the original BSIM4, it still results in larger simulation errors than the new one at  $V_{dg} < -V_{th}$  as a result of (5).

As a result, the new model shows the best agreement with measured one than the conventional models.

### III. Conclusions

The inaccuracy of the original BSIM4 and BSIM4 macro model using a diode is revealed in detail. In order to get rid of the inaccuracy, a physical

bias-dependent  $C_{gdo}$  equation for N-MOSFETs is derived by modeling a parasitic MOS capacitor using the series connection of  $C_{OLD}$  and  $C_{de}$  with the paralleled  $C_{pgd}$  in the gate-drain overlap region. Unlike the conventional models, a new BSIM4 macro model with the  $C_{gdo}$  equation is able to accurately model C-V characteristics at full bias region. This new model is demonstrated by observing much better agreements with measured power gain versus frequency than that of the original BSIM4.

### REFERENCES

- [1] J. Cha, J.-Y. Cha, and S. Lee, "Analysis of fT and fmax dependent on unit gate finger width for RF performance optimization of MOSFETs," Journal of The Institute of Electronics Engineers of KOREA - Semiconductor and Devices, vol. 45, no. 9, pp. 21-24, 2008.
- [2] BSIM4.8.0 MOSFET Model Manual, U. C. Berkeley, 2013.
- [3] S. Lee, C. S. Kim, H.-K. Yu, "Large-signal MOSFET modeling and parameter extraction for high-frequency IC design," Telecommunication Review, vol. 12, no. 1, pp. 130-137, Feb. 2002.
- [4] J.-Y. Kim, M.-K. Choi, and S. Lee, "A "Thru-Short-Open" deembedding method for accurate on-wafer RF measurements of nanoscale MOSFETs," Journal of Semiconductor Technology and Science, vol. 12, no. 1, pp. 53-58, Mar 2012.
- [5] S. Lee, "Accurate RF extraction method for resistances and inductances of sub-0.1 $\mu$ m CMOS transistors," Electron. Lett., vol. 41, no. 24, pp. 1325-1327, Aug 2005.
- [6] J. Kim, Y. Lee, M. Choi, J. Ku, and S. Lee, "Gate-length dependent cutoff frequency extraction for nano-scale MOSFET," Journal of The Institute of Electronics Engineers of KOREA - Semiconductor and Devices, vol. 42, no. 12, pp.1-7, 2005.
- [7] H.-J Lee and S. Lee, "Extraction method for non-quasi-static gate resistance of RF MOSFETs," Electron. Lett., vol. 48, no. 23, pp. 1501-1503, Nov 2012.
- [8] Star-Hspice Manual, Avant! Corporation, 1998.
- [9] N. Arora, MOSFET Modeling for VLSI

Simulation, World Scientific, Singapore, 2007.

- [10] J.-Y. Kim, M.-K. Choi, and S. Lee, "Accuracy analysis of extraction method for effective channel length in deep-submicron MOSFETs," Journal of Semiconductor Technology and Science, vol. 11, no. 2, pp. 130-133, June 2011.
- [11] J.-Y. Kim, B.-H. Ko, M.-K. Choi, and S. Lee, "RF extraction method for source/drain overlap and depletion length of deep-submicron RF MOSFETs using intrinsic gate-bulk capacitance," Electron. Lett., vol. 46, no. 23, pp. 1566-1568, Nov. 2010.

---

저 자 소 개

---



이 상 준(학생회원)  
2012년 고려대학교 전자 및 정보  
공학과 학사 졸업.  
2013년 ~ 현재 한국외국어대학교  
전자정보공학과 석사과정.  
<주관심분야 : RF CMOS 소자  
모델링>



이 성 현(정회원)-교신저자  
1985년 고려대학교 전자공학과  
학사 졸업.  
1989년 미국 University of  
Minnesota 전기공학과  
석사 졸업.

1992년 미국 University of Minnesota  
전기공학과 박사 졸업.

1992년 ~ 1995년 한국전자통신연구원 선임연구원  
1995년 ~ 현재 한국외국어대학교 전자공학과  
교수

<주관심분야 : CMOS 및 바이폴라 소자 모델링>